An Investigation of the Breakup Mechanisms for Swirl Sprays From High-Pressure Swirl Injectors

Chryssakis C.[1*], Assanis D.[1], Lee J.[2], Nishida K.[2]

1. University of Michigan, 1231 Beal Ave., Ann Arbor, MI 48109, U.S.A.
2. University of Hiroshima, 1-4-1 Kagamiyama, Higashi-Hiroshima 739-8527, Japan

A computational model for swirl sprays from inwardly opening swirl injectors used in direct-injection gasoline engines has been developed, accounting both for primary and secondary breakup processes. Good agreement is demonstrated for the main part of the spray under atmospheric pressure. However discrepancies occur for higher ambient pressures and for the pre-swirl spray under atmospheric pressure. An in-depth analysis of pre-spray and high pressure results is presented here in an attempt to explain the causes of these discrepancies and suggest ways to improve the current breakup models.

1. Introduction

High-Pressure Swirl (HPS) sprays, emerging from inwardly opening HPS injectors, are typically used in Direct-Injection Spark-Ignition (DISI) engines. HPS injectors operate at relatively high injection pressures (4-12 MPa) and their design enhances atomization as well as turbulence levels in the cylinder for a more efficient combustion process. Instead of the round jet solid-cone structure common to diesel injectors, the HPS injector produces a hollow-cone spray structure by providing a strong swirl motion to the fuel inside the injector. The development of the spray emerging from an HPS injector can be divided into two phases: the transient phase at the beginning of injection and the steady-state phase that corresponds to the largest part of the injection process. Upon the start of injection, due to the lack of high swirl, a solid-cone-like structure appears with narrow cone angle and relatively large droplets. As the fuel velocity inside the nozzle increases, the angular momentum and the centrifugal forces increase too, thus forcing the fuel to form a hollow-cylinder structure, adjacent to the walls of the nozzle, which transforms into a hollow-cone as the fuel emerges in the combustion chamber.

Numerical models have been proposed based on empirical constants that can be adjusted according to the specific conditions and give reasonably accurate results for typical sprays encountered in DISI applications. A number of primary atomization models have been suggested [1-4] in order to provide initial conditions for the secondary atomization. The secondary atomization process is commonly modeled using Lagrangian particle tracking techniques, based on experimental observations and simplifying assumptions [5-8].

It has been found in previous work by the authors [9,10] that predictions for a spray emerging from an HPS atomizer are in good agreement with experimental observations for the main part of the spray under atmospheric conditions. However, the pre-swirl spray tip penetration and droplet sizes are strongly underestimated when the same secondary breakup model is used for both parts of the spray. In the same work it has been verified that current breakup

* Corresponding author (cchryssa@umich.edu)

models are not performing in a satisfying manner under high ambient pressures representative of realistic engine conditions. An in-depth analysis of the results obtained in [10] is presented here in an attempt to explain the causes of these discrepancies and suggest ways to improve the current breakup models. It will be shown that in these sprays more than one secondary breakup mode plays a significant role in the atomization process and a simplified model cannot account for the phenomena occurring during breakup of the different parts of the spray. Distinction between various breakup regimes is not always well established in the current models. There are four breakup regimes of interest in common gasoline sprays [11-14] that should be taken into account, depending on the Weber and Ohnesorge number of the drops. A further feature that will be examined here is the duration of the breakup process. Most models impose breakup, resulting drop size and velocity distributions as jump conditions, while in reality breakup times are incrementally larger than computational time steps [11-14] and thus breakup processes should be approached as functions of time.

2. Description of the Computational Spray Model

A comprehensive model for sprays emerging from high-pressure swirl injectors in DISI engines has been developed accounting for both primary and secondary atomization [9,10]. The model considers the transient behavior of the pre-swirl spray and the steady-state behavior of the main spray. The pre-swirl spray modeling is based on an empirical solid-cone approach with varying cone angle. First, a solid-cone-like injection is performed, representing the pre-swirl spray and the cone angle is gradually being increased, using a linear profile. After some point, defined by the user in the input file, the code switches into a hollow-cone structure, while the cone angle is still increasing until the steady-state value is reached. In addition, a new velocity profile has been added to KIVA, allowing for gradually increasing injection velocity during the start-up injection period.
The primary breakup approach adopted here for the main spray is based on the Linearized Instability Sheet Atomization (LISA) model [3,4], with appropriate extensions to include a swirl velocity component. The main part of the model has been retained and is being used to estimate the liquid sheet breakup length, the breakup time and the initial droplet size. The computed mean drop diameter from the LISA model is assumed to represent the SMD of the droplet parcels introduced at the liquid sheet break-up length and a Rosin-Rammler cumulative distribution is used in this work. For the secondary droplet breakup the TAB model [5] is being used both for the pre-swirl and the main spray, with its baseline constants.

3. Experimental Techniques

A complete set of data for spray model validation purposes has been acquired using LIF, PIV, Mie Scattering, and Laser Droplet Size Analyzer (LDSA) techniques to characterize a High-Pressure Swirl Injector. The measurements have been obtained in an optical static cell, with size 10×10×10 cm. The experimental conditions are given in Table 1. The ambient gas is Nitrogen (N_2). A non-evaporating dry solvent is used as the fuel. The injection pressure is 5 MPa, the injection duration 1.25 ms, the injected quantity 7.24 mg/inj. and the spray cone angle under atmospheric pressure is 50^o. Ambient pressures of 0.1 and 0.4 MPa have been employed and the ambient temperature was kept constant at 293 K. More details on the experimental apparatus are given in [10].

4. Comparison of Experimental Measurements and Predictions

4.1. Computational Initial and Boundary Conditions

For the numerical simulations performed here KIVA-3V [15-17] has been used as the modeling framework. The spray droplets are represented by 5,000 computational parcels, each one containing droplets with the same properties. Isooctane (n-C_8H_{18}) has been used as a fuel in the computations, with properties slightly different than the ones of the dry-solvent used in the experiments. The collision model has been deactivated, in order to investigate the behavior of the breakup model. The computational grid consists of a 3-D representation of the optical static cell used in the experiments, with homogeneous computational cells with size of 2.4 mm, which is typical of the grids used in engine simulations.

4.2. Free-Spray Comparison

A qualitative comparison of the observed and predicted spray structure is presented in Figure 1, where five different snapshots are shown at 0.2 ms, 0.5 ms, 0.8 ms (first row), and at 1.3 ms and 1.8 ms (second row) after the Start Of Injection (SOI). The scale is given on the left of each row, with a 60×30 mm and a 75×40 mm domain of the computational grid and the static cell illustrated for comparison of the experiments with the model for the first and the second row, respectively. The left part of each image shows a spray tomogram, obtained with a PIV technique. On the right hand side, the discrete computational parcels used in the numerical simulations are shown.

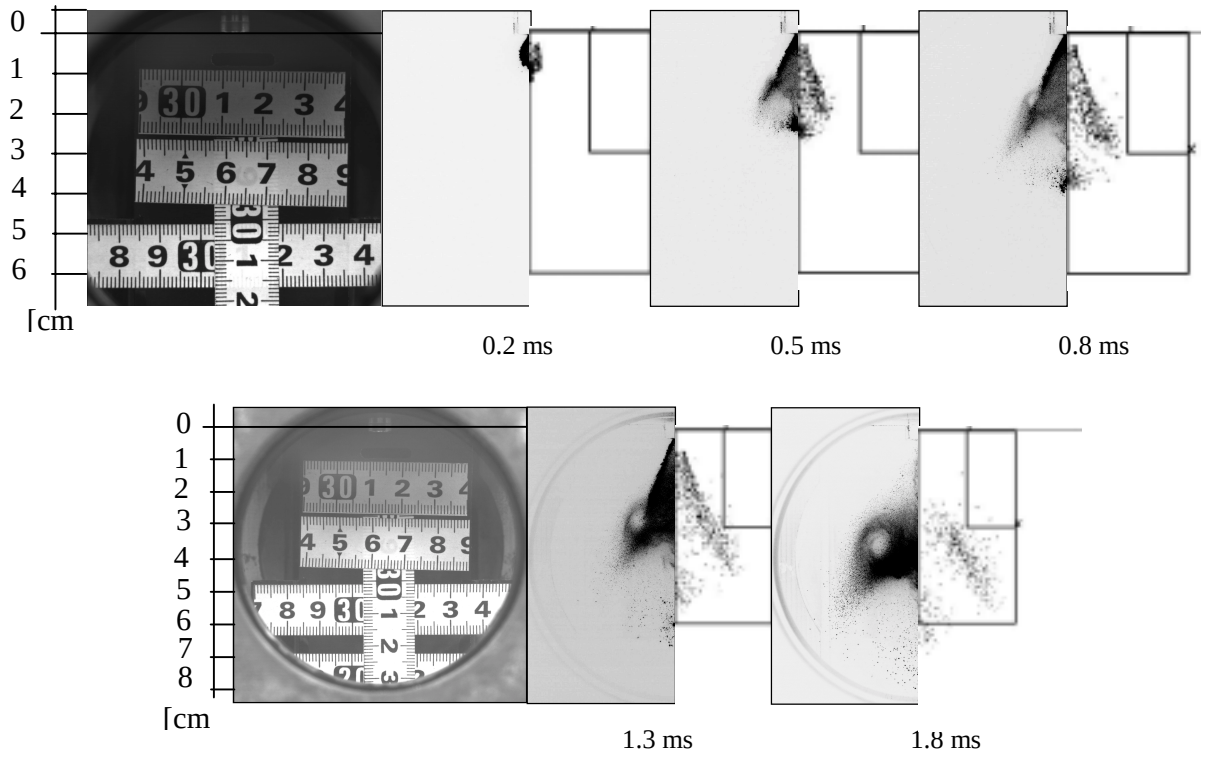

Figure 1: Comparison of Spray Tomograms (left) with KIVA-3V computational parcels (right) at various instants, under ambient pressure (0.1 MPa).

Overall, the snapshots shown in the first row indicate reasonably good predictions of both the pre-swirl and the main spray features. In the second row, where the pre-swirl spray has moved farther away from the main spray, it appears that the model can only predict correctly the main spray structure.
More insight on the behavior of the model can be gained if the calculated SMD is compared to the experimental measurements at two planes located 27 mm and 36 mm downstream of the injector, as shown in Figure 2(a). In order to ensure the presence of a sufficient number of computational parcels at a given plane to produce statistically meaningful SMD results, the sampling was done within planes located ±2 mm of the specified location. While the SMD predictions agree almost perfectly with measurements for late timings, the droplet sizes are strongly underestimated for early timings. This can be explained by the fact that for early timings only the pre-swirl spray has reached the planes of interest. Additional runs have been performed for injection under ambient pressure of 0.4 MPa. As shown in Figure 2(b), where the measured and predicted tip penetrations of the pre-swirl spray and main spray are plotted against time, the comparison is not satisfactory. Initially, the penetration of the pre-spray is slightly overestimated, but as injection proceeds, it is strongly underestimated. Similarly, the penetration of the main spray is underestimated.

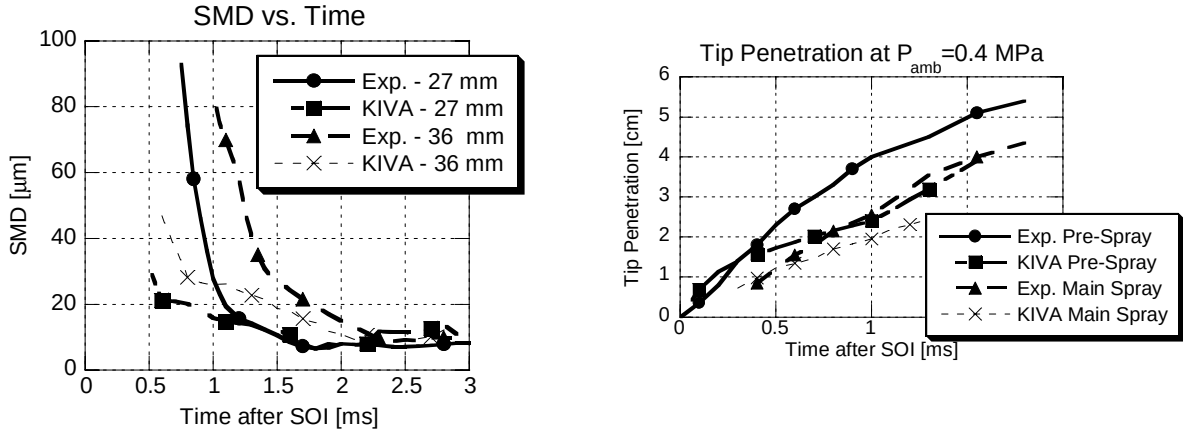

Figure 2: (a) SMD versus time for ambient pressure 0.1 MPa, (b) Tip penetration for ambient pressure 0.4 MPa.

5. Analysis of Results and Exploration of Breakup Regimes

5.1. General Observations

Inspection of Figures 1 and 2 reveals that the current model performs well for the main-spray under atmospheric conditions. However, under higher ambient pressures it fails to provide a reliable representation of the spray structure. In addition, the pre-swirl spray is not adequately modeled, even under atmospheric conditions. Likely causes for the discrepancies include the facts that (i) the primary atomization process is not adequately captured (droplet sizes, break-up length, time), (ii) the secondary atomization model breaks up parent droplets excessively or (iii) the aerodynamic drag is overestimated, thus opposing droplet penetration. This suggests that additional effort needs to be undertaken to understand, model and validate the mechanisms of droplet break-up under higher ambient pressures.

5.2. Primary Breakup of the Pre-Swirl Spray

The primary breakup mechanism of the pre-swirl spray has been experimentally investigated using an Image Processing technique developed by Lee & Nishida [18]. In Figure 3 images taken at 0.25-0.65 ms after the start of injection (SOI) are presented. It is apparent that big blobs and ligaments are present until about 0.6 ms after SOI, indicating that the primary atomization process comes to an end at this time instant and secondary atomization considerations can only start after this timing. Failure to take into account this time delay in the original model leads to pre-swirl spray drops atomizing sooner than in reality, resulting in significantly smaller drop sizes and, consequently, shorter penetration lengths.

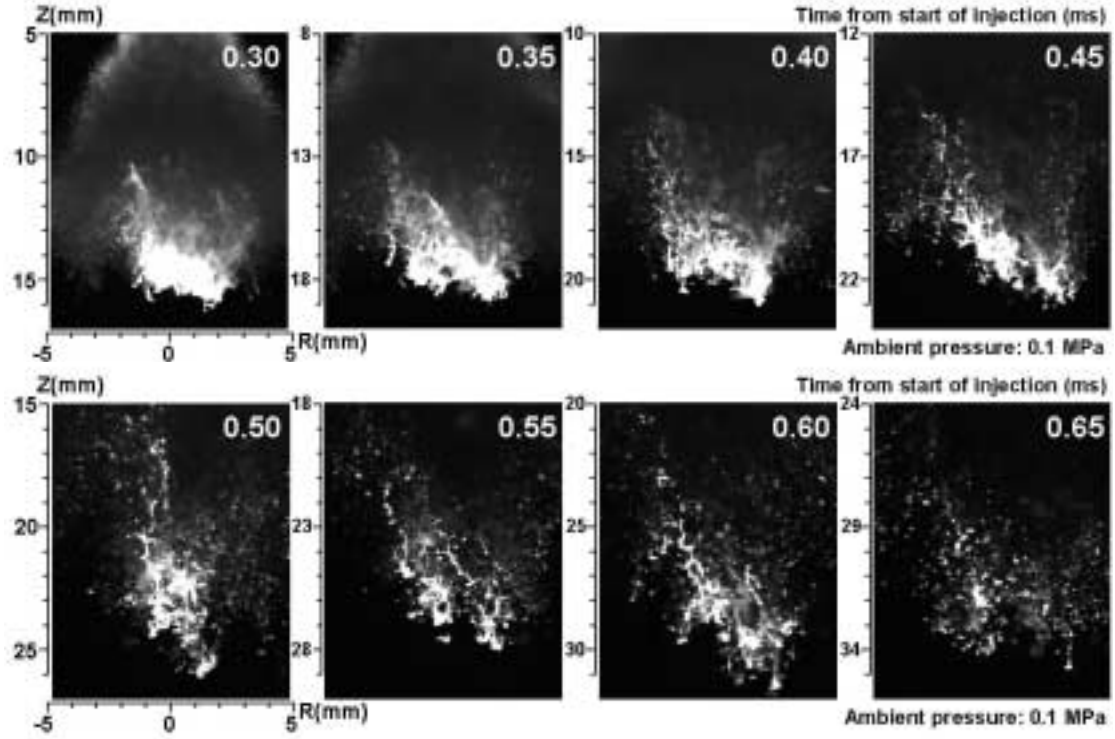

Figure 3: Pre-swirl spray primary atomization, ambient pressure 0.1 MPa.

5.3. Secondary Breakup Regimes

The breakup regimes applying on the conditions met by the sprays under investigation have been determined using the classification by Faeth et al. [12-14], according to which four main domains are important for droplet deformation and breakup. The regimes have been defined as functions of the Weber (*We*) and Ohnesorge (*Oh*) numbers of the droplets upon their creation after the end of primary breakup, following the methodology first proposed by Hinze [19] in 1955, where

$$We = \frac{\rho_G U^2 d}{\sigma} \text{ and } Oh = \frac{\mu_L}{(\rho_L d\sigma)^{1/2}}. \quad (1)$$

For $Oh \ll 1$ the values of *We* at the transitions are relatively independent of *Oh*, indicating that aerodynamic forces can only be stabilized by surface-tension forces when liquid-viscous forces are small. The four regimes of importance are (i) oscillatory deformation, $We<12$, (ii) bag breakup, $12<We<35$, (iii), multimode, $35<We<80$ and (iv) shear, $80<We<850$. It is particularly interesting to determine the breakup regimes of the spray droplets for a range of ambient pressures. This is shown in Figure 4a, where the *We* and *Oh* of individual droplets re-

sulting from primary atomization are plotted, both for the pre-swirl and the main spray, for ambient pressure of 0.1 and 0.4 MPa, as estimated by KIVA. In Figure 4b the experimental measurements presented in Figure 3 are plotted for the pre-swirl spray. It is interesting to note that in all cases Oh<0.1, hence the transitions between regimes occur at constant We. The experiments show that the pre-swirl spray mainly consists of drops with low We, as opposed to the assumption of very high We used at the simulations. This is illustrated in Figure 5, where drop size distributions are plotted, comparing the initial drop sizes in KIVA with data measured at various timings in the experiment. Initially, a small number of very large blobs have been measured, which is progressively being transformed into a larger number of smaller spherical drops. Secondary atomization is estimated to start at around 0.7-0.8 ms after the start of injection, when the drop sizes are distributed around a value of approximately 50 μm. In contrast, in KIVA it is assumed that secondary atomization starts immediately and the drop sizes are distributed around a value of almost 500 μm, which is an order of magnitude larger than the experimentally measured drop sizes. This occurs because it is assumed that the initial diameter of the pre-swirl spray drops is equal to the orifice diameter and explains why the We number is almost an order of magnitude higher than the experimental one, leading to very intense atomization in the computations. Detailed experimental measurements for the main spray are not available but they would offer precious insight for the high ambient pressure case.

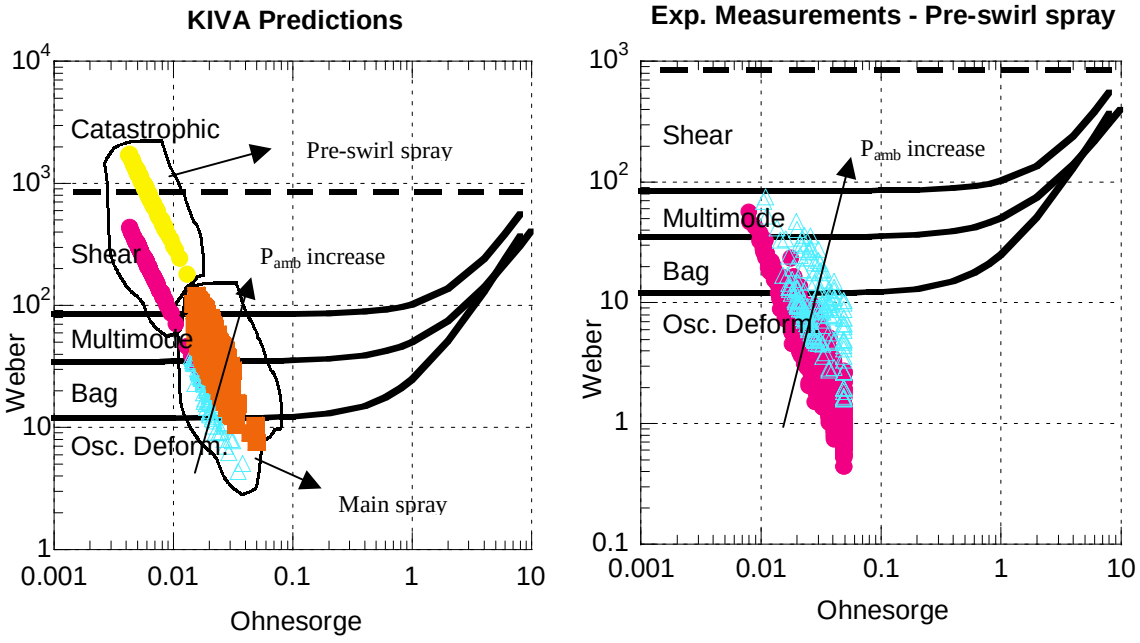

Figure 4: (a) KIVA characterization of pre-swirl and main spray droplets resulting from primary atomization in relation to secondary breakup regimes (b) Experimental measurements of the pre-swirl spray relative to secondary breakup regimes.

A further observation is that as ambient pressure increases, We increases as well, due to its dependency on the ambient gas density. This implies that for high ambient pressures a computational model considering only the bag breakup regime cannot be used. The spray comparisons shown in Figure 1 and 2 indicate that only the main spray, under atmospheric conditions, is in good agreement with experiment, suggesting that the TAB model only performs well in the bag breakup regime, since the bulk of the droplets under 0.1 MPa conditions are in this regime. Under higher ambient pressures the multimode and, in the limit, the shear breakup regime become also important. It is expected that in even higher ambient pressures

(1.0 MPa) the shear breakup will be the dominant mechanism. In this case a breakup model that accounts for all three regimes should be used.

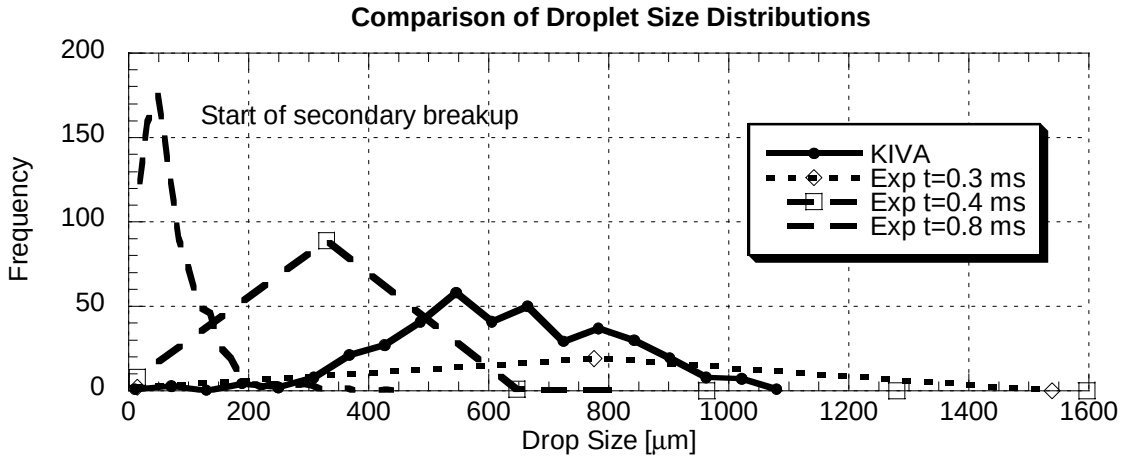

Figure 5: Comparison of predicted and measured drop size distributions at various timings.

5.4. Breakup Times

Another significant aspect of the secondary atomization process is the initiation and end of breakup time. A simple empirical correlation is proposed [11] that adequately describes the breakup initiation time for both low and high Ohnesorge numbers:

$$\frac{t}{t^*} = 1.9 \cdot (We - 12)^{-1/4} \left(1 + 2.2 Oh^{1.6}\right), \tag{2}$$

where t^* is a dimensionless time characteristic of drop breakup, proposed by Ranger & Nicholls [20] as:

$$t^* = \frac{d_o}{u_o}\left(\frac{\rho_L}{\rho_g}\right)^{1/2}. \tag{3}$$

Total breakup is defined as the time when the drop (if a coherent drop exists) and all its fragments no longer undergo further breakup. Correlations for total breakup time are given by Pilch & Erdman [11]:

$$t/t^* = 6(We-12)^{-1/4}, \quad 12<We<18 \tag{4a}$$
$$t/t^* = 2.45(We-12)^{1/4}, \quad 18<We<45 \tag{4b}$$
$$t/t^* = 14.1(We-12)^{-1/4}, \quad 45<We<351 \tag{4c}$$
$$t/t^* = 0.766(We-12)^{1/4}, \quad 351<We<2670 \tag{4d}$$

In Figure 6, the breakup times predicted by the TAB model are plotted along with values predicted by correlations (4a-d). It seems that the TAB model predicts the onset of breakup with good accuracy for low *We* but provides longer estimates than suggested from experiments for larger *We*. Over the entire *We* range, drops are predicted to break up instantaneously, whereas in reality a much longer time is required for the process to be completed, particularly in large *We* numbers. Additionally, the primary breakup time is not considered in the computational model for the pre-swirl spray, leading to very fast atomization rates and very small droplet sizes. The small droplet sizes also result in under-predicting the penetration of pre-swirl sprays, as demonstrated in Figures 1 and 2.

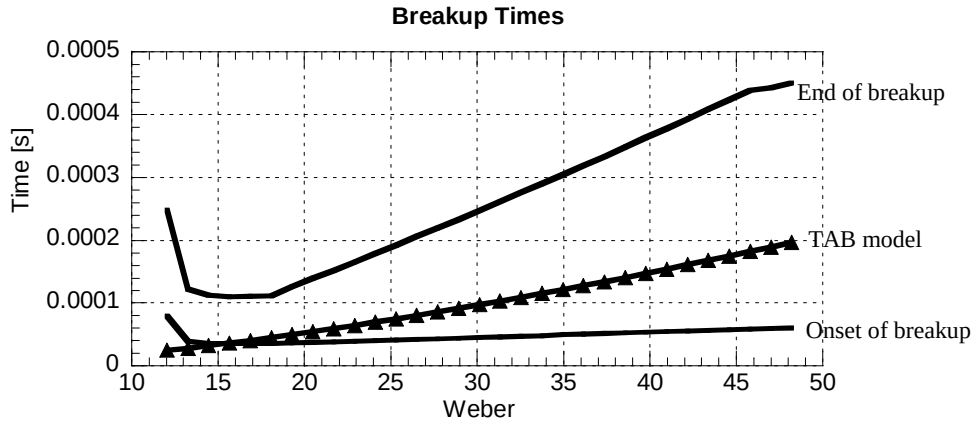

Figure 6: Secondary breakup times, theoretical and predicted.

6. Conclusions

The primary and secondary breakup processes for the pre-swirl spray of a spray emerging from a HPS injector have been investigated by comparing KIVA predictions with detailed experimental data acquired with laser diagnostic techniques. It is concluded that the primary breakup for the pre-swirl spray is considerably long and should not be ignored. Also, the *We* for the pre-swirl spray is strongly overestimated in KIVA leading to incorrect atomization rates. This can be corrected by introducing a primary breakup process for the pre-swirl spray, during which the drops will not be subject to breakup according to the secondary atomization models. It is anticipated that a model considering more than one breakup mechanisms should be employed in order to accurately predict spray behavior under high ambient pressures.

7. References

[1] Dorfner V., Domnick J., Durst F., Koehler R., *Atomization and Sprays* **5** 261-285, 1995
[2] Han Z., Parrish Sc., Farell P.V., Reitz R.D., *Atomization and Sprays* **7** 663-684, 1997
[3] Schmidt D.P. et al., Martin J.K., Reitz R.D., *SAE 1999-01-0496,* 1999
[4] Senecal P.K. et al., *Int. J. of Multiphase Flow* **25**, 1073-1097, 1999
[5] O'Rourke P.J., Amsden A.A., *SAE 872089*, 1987
[6] Reitz R.D., Diwakar R., *SAE 870598*, 1987
[7] Tanner F.X., *SAE 970050*, 1997
[8] Ibrahim E.A. et al.,*J. Propulsion Power* **9**, 651-654, 1993
[9] Chryssakis C.A., Driscoll K.D., Sick V., Assanis D.N., *ILASS-Europe*, 2002
[10] Chryssakis C.A., Assanis D.N., Lee J.-K., Nishida K., *SAE 2003-01-0007*, 2003
[11] Pilch M., Erdman C.A., *Int. J. Multiphase Flow*, **13**, No. 6, 741-757, 1987
[12] Hsiang L.-P., Faeth G.M., *Int. J. Multiphase Flow* **18**, No. 5, 635-652, 1992
[13] Faeth G.M., Hsiang L.-P., Wu P.-K. *Int. J. Multiphase Flow* **21**, 99-127, 1995
[14] Hsiang L.-P., Faeth G.M., *Int. J. Multiphase Flow* **21**, No. 4, 545-560, 1995
[15] Amsden A.A. et al., *Los Alamos National Lab. LA-11560-MS*, 1989
[16] Amsden A.A., *Los Alamos National Lab.* LA-12503-MS, 1993
[17] Amsden A.A., *Los Alamos National Lab., LA-13313-MS*, July 1997
[18] Lee J., Nishida K., *ICLASS 2003*, Italy, 2003
[19] Hinze J.O., *AIChE* **1**, 289-295, 1955
[20] Ranger, A.A., and Nichols, J.A., *AIAA* **7**, 285-290, 1969